Heading Drift Reduction for Foot-Mounted Inertial Navigation System via Multi-Sensor Fusion and Dual-Gait Analysis

Hongyu Zhao, Zhelong Wang, *Senior Member, IEEE*, Sen Qiu, Yanming Shen, Luyao Zhang, Kai Tang, and Giancarlo Fortino, *Senior Member, IEEE*

***Abstract*— Foot-mounted inertial navigation is an important issue in areas such as pedestrian localization, gait analysis, and sport training. However, low-cost inertial sensors suffer from several errors that make the navigation results less convincing. In this paper, a multi-sensor approach with one sensor on each foot is presented to reduce the system heading drift. Through dual-gait analysis, gait parameters between two feet are employed to make the non-collocated and uncoupled subsystems be related to each other. A step length estimator based on an inverted pendulum model is developed to derive a relative position vector between the two foot-mounted sensors rather than a distance scalar. A Kalman-type filter with one time update and two measurement updates is developed to fuse the velocity and position observations at foot and person levels, respectively. Experiments were conducted by four healthy subjects, and experimental results show that the proposed sensor fusion method can effectively reduce the heading drift of inertial navigation and make the captured dual-foot motion closer to its actual process.**

***Index Terms*— Dual-gait analysis, multi-sensor fusion, foot-mounted inertial navigation system (INS), inertial measurement unit (IMU), zero velocity updates (ZUPT).**

I. Introduction

THERE is an increasing demand for a portable and accurate pedestrian navigation system that works in both indoor and outdoor environments [1]–[3]. The commonly used GPS does not work everywhere, especially the indoor environments where people spend most of their time. Several technologies are being developed to achieve a non-GPS solution, some of which involve the use of Wi-Fi or Ultra-Wideband (UWB) signals [4], [5]. The accuracies achieved by these technologies vary from a few centimeters to a few meters. However, in some harsh environments, e.g., a fire-affected building where one has to locate the fire fighters rushing into the scene to carry out their mission, the assumption of existing infrastructure developments like Wi-Fi or UWB network cannot be satisfied. Therefore, there is a need for infrastructure-free navigation systems.

Manuscript received May 31, 2018; revised August 2, 2018 and August 14, 2018; accepted August 20, 2018. Date of publication August 23, 2018; date of current version September 5, 2019. This work was supported in part by the China Postdoctoral Science Foundation under Grant 2017M621131, in part by the Fundamental Research Funds for the Central Universities under Grants DUT18RC(4)036 and DUT16RC(3)015, and in part by the National Natural Science Foundation of China under Grant 61473058. The associate editor coordinating the review of this paper and approving it for publication was Prof. Mehmet Yuce. *(Corresponding author: Hongyu Zhao.)*

H. Zhao is with the School of Control Science and Engineering and the School of Computer Science and Technology, Dalian University of Technology, Dalian 116024, China (e-mail: zhaohy@dlut.edu.cn).

Z. Wang, S. Qiu, and L. Zhang are with the School of Control Science and Engineering, Dalian University of Technology, Dalian 116024, China (e-mail: wangzl@dlut.edu.cn; qiu@dlut.edu.cn).

Y. Shen is with the School of Computer Science and Technology, Dalian University of Technology, Dalian 116024, China (e-mail: shen@dlut.edu.cn).

K. Tang is with the First Affiliated Hospital of Dalian Medical University, Dalian 116024, China (e-mail: dltangkai@126.com).

G. Fortino is with the Department of Informatics, Modeling, Electronics, and Systems, University of Calabria, 87036 Cosenza, Italy (e-mail: g.fortino@unical.it).

Digital Object Identifier 10.1109/JSEN.2018.2866802

As an autonomous solution, Inertial Navigation System (INS) works in almost all environments [6]. The development of Microelectromechanical System (MEMS) and Body Sensor Networks (BSN) has facilitated this application [7], [8]. INSs constructed of MEMS Inertial Measurement Unit (IMU) can be considered as a potential alternative to GPS or a possible complement to GPS. However, for inertial navigation purposes, the measurements must be numerically integrated to provide the information of attitude, velocity and position. This mechanization makes INS prone to errors, as any small error will accumulate and grow without bound due to the successive integration, especially when using low-cost MEMS IMUs, which typically have large bias drifts [9]. Therefore, the main challenge in developing an autonomous navigation system is to ensure a sufficient accuracy.

A preferred location of IMU for pedestrian navigation is the user's shoe, as it is the nature of walking or running that foot swings to stance phase every gait cycle and then shows a zero velocity until the foot swings again. This information can be used by the Zero Velocity Update (ZUPT) technique to reset the accumulated navigation errors [10]. However, although the errors in the foot-mounted INS can be bounded via ZUPT, the position and heading errors are unobservable and grow without bound. To reduce the error growth further, dual-sensor approach (as illustrated in Fig. 1) with one sensor on each foot seems to be a promising way, as suggested early in [11].

Since human body is non-rigid, the relative position between the uncoupled foot-mounted INSs is unknown, but it relates to the spatial gait parameters with knowledge of human gait. Although the navigation results of one foot cannot be directly related to the other, there exists an upper bound on how far apart they could be, and this information can be fused to mitigate the ever-increasing heading drift. Thus, the fusion of the two navigation solutions is often regarded as a fusion problem with nonlinear inequality constraints.

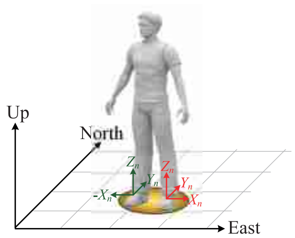

Fig. 1. Dual-sensor configuration for pedestrian navigation.

Several methods have been developed to solve the dual-sensor fusion problem [12]. An extended Kalman filter (EKF) is used in [13] to fuse the position estimates with anthropometric considerations specific to the user biomechanics. A spherical constraint method is proposed in [14] based on the idea that the relative position between two feet must always be within a sphere with radius equal to their maximum spatial separation. A projection method is proposed in [15] based on an inequality constrained least square problem formulation. A centroid method is proposed in [16] under the same constrained least squares framework by applying the constraint at all-time instants. A Bayesian inference method is proposed in [17] by posing the constraint problem in a Bayesian framework. Moreover, as suggested in [18], to make the range constraint more precise, the constraint should have different values in the horizontal and vertical directions rather than a spherical model. An ellipsoidal constraint model that relates to the maximum step length and the leg height is recommended in [19].

Although the above methods can greatly reduce the heading drift, more work can be done to further improve the system performance, as there still exists a number of shortcomings: (1) the spatial feet separation is constrained by an empirically predefined upper bound (e.g., 1 m in [15] and [16]), which is unadaptable and conservative; (2) the spherical or ellipsoidal constraint does not take the walking direction into consideration, making the constraint to have the same extend in the forward and lateral directions, which may result in the feet trajectories of one person having a lateral separation equal to the upper bound after even a few seconds.

As suggested in [20], the spatial constraint between two feet can be either a distance scalar or a position vector. The latter suggestion decomposes the constraint along three orthogonal directions, which is more accurate and supposed to yield better results. The forward component is the so-called step length, which varies considerably with gait pattern and needs to be calculated separately for each step of each individual. The step length can be used as a position observation for fusing the information from the two foot-mounted INSs.

Many methods have been developed to estimate the step length with a mathematical model. A single inverted pendulum model is employed in [21] with two sensors fixed on shank and thigh segments. A double pendulum model is presented in [22] with three sensors attached on shank segments and right thigh. A four-sensor configuration is proposed in [23] with the sensors placed on shanks and thighs. Comparisons of different step length estimators are presented in [24] and [25]. Generally, the gait model can be driven by different combinations of direct or indirect, accelerometer or gyroscope measurements, with the sensors placed on shank, thigh or lower lumbar spine closer to the body's center of mass (COM). To comply with the sensor configuration in Fig. 1, this paper makes some modifications to the existing methods [21]–[23], and a step length estimator with one sensor on each foot is developed.

This paper aims to reduce the heading drift of foot-mounted INS via multi-sensor fusion and dual-gait analysis. To our knowledge, although several multi-sensor approaches have been developed for pedestrian navigation [13]–[20], no studies have been reported on the implementation and application of dual-gait analysis for the multi-sensor fusion. The dual-gait analysis has two main advantages: (1) at foot level, it can provide better gait detection results than single-gait analysis, which helps to delimit the ZUPT periods and makes the zero velocity information more reliable, so as to improve the accuracy of each ZUPT-aided INS; (2) at person level, it can represent the feet separation by three vector components rather than a distance scalar, which not only makes the non-collocated and uncoupled foot-mounted INSs be related to each other, not also makes the relative position information more specific and accurate without resorting to other ranging technology (e.g., RF [11] or ultrasonic [26]).

Therefore, a Kalman-type filter with one time update and two measurement updates is developed in this paper. Among the two measurement updates, one is aided with the zero velocity observation at foot level, whereas the other is aided with the relative position observation at person level. The proposed sensor fusion method is evaluated with experimental data, and the results show that the heading drift of foot-mounted INSs is effectively reduced, and thereby making the captured dual-foot motion closer to its actual process.

II. ZUPT-Aided INS Without Position Updates

Without applying any constraint on the feet separation, each foot-mounted INS runs independently and is aided by merely ZUPT. The ZUPT-aided INS presented in this paper has four main modules: sensor model, INS module, gait detection module, and error estimation module, as described below.

A. INS Mechanization Equation

For an initial calibration, the system was kept stationary and the known ground truths are: (1) the angular rate is zero around each axis; (2) the magnitude of specific force equals the magnitude of gravitational acceleration. During a stationary period lasting about 8 seconds, the angular rate and the magnitude of specific force are shown in Fig. 2, where the bias error of gyroscope and the scale factor error of accelerometer can be identified. The sensor model corrects the IMU measurements by compensating for these errors.

In practical applications, due to the limited speed and range of foot motion, as well as the poor error characteristics and high sampling rates of low-cost IMUs, the full INS equations can be simplified by ignoring some physical effects, such as the Earth's rotation and curvature, the Coriolis force, and the centrifugal force. Therefore, based on the error-compensated IMU measurements, simplified INS equations are used to yield

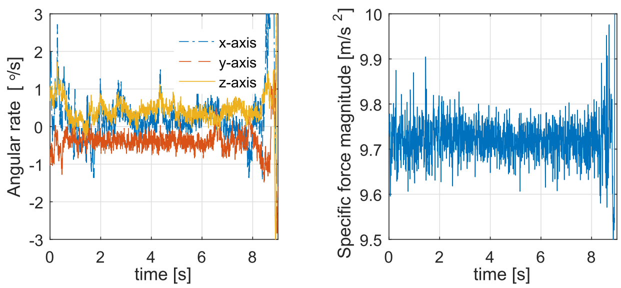

Fig. 2. Raw inertial measurements during a stationary calibration period.

the navigation solution as

$$\begin{aligned} \dot{\boldsymbol{C}}_b^n &= \boldsymbol{C}_b^n \boldsymbol{\Omega}_{ib}^b \\ \dot{\boldsymbol{v}}^n &= \boldsymbol{C}_b^n \boldsymbol{f}^b + \boldsymbol{g}^n \\ \dot{\boldsymbol{p}}^n &= \boldsymbol{v}^n, \end{aligned} \tag{1}$$

where n denotes the navigation coordinate frame (n-frame for short), b denotes the body coordinate frame (b-frame for short), i denotes the inertial coordinate frame; $\boldsymbol{C}_b^n$ is the rotation matrix transforming from the b-frame to the n-frame, $\boldsymbol{v}^n$ is the velocity, $\boldsymbol{p}^n$ is the position; $\boldsymbol{\Omega}_{ib}^b$ is the skew-symmetric matrix of the angular rate $\boldsymbol{\omega}_{ib}^b$ measured by gyroscope, $\boldsymbol{f}^b$ is the specific force measured by accelerometer, $\boldsymbol{g}^n$ is the gravity.

Define $\boldsymbol{\varphi}$ be the Euler angle vector equivalent to the rotation matrix $\boldsymbol{C}_b^n$, then the state vector of each INS can be defined as $\boldsymbol{x}_k = \left[\boldsymbol{\varphi}_k, \boldsymbol{v}_k^n, \boldsymbol{p}_k^n\right]^T \in \mathbb{R}^9$. Note that the INS mechanization only yields a raw navigation solution, which is updated by the latest IMU measurements but not corrected for any errors yet.

B. Kalman Filter-Based ZUPT

The gait detector uses the IMU measurements to generate a logic signal for activating the ZUPT when the foot is in its stance phase. When the ZUPT is activated, a Kalman-type filter acts as an indirect filter to estimate the errors of the raw INS states. The process model is designed based on a simplified INS error model

$$\begin{aligned} \delta\dot{\boldsymbol{\varphi}} &= -\boldsymbol{C}_b^n \delta\boldsymbol{\omega}_{ib}^b \\ \delta\dot{\boldsymbol{v}}^n &= (\boldsymbol{C}_b^n \boldsymbol{f}^b) \times \delta\boldsymbol{\varphi} + \boldsymbol{C}_b^n \delta\boldsymbol{f}^b \\ \delta\dot{\boldsymbol{p}}^n &= \delta\boldsymbol{v}^n, \end{aligned} \tag{2}$$

where $\delta\boldsymbol{\varphi}$ is the attitude error, $\delta\boldsymbol{v}^n$ is the velocity error, $\delta\boldsymbol{p}^n$ is the position error, $\delta\boldsymbol{\omega}_{ib}^b$ and $\delta\boldsymbol{f}^b$ are the measurement errors of the gyroscope and accelerometer respectively.

Define the error vector as $\delta\boldsymbol{x}_k = \left[\delta\boldsymbol{\varphi}_k, \delta\boldsymbol{v}_k^n, \delta\boldsymbol{p}_k^n\right]^T \in \mathbb{R}^9$, the discrete state space model can be expressed as

$$\begin{aligned} \delta\boldsymbol{x}_k &= \boldsymbol{F}_k \cdot \delta\boldsymbol{x}_{k-1} + \boldsymbol{w}_{k-1} \\ z_{v,k} &= \boldsymbol{H}_v \cdot \delta\boldsymbol{x}_k + \boldsymbol{\eta}_{v,k}, \end{aligned} \tag{3}$$

where k is the time instant, $\boldsymbol{F}_k$ is the state transition matrix, $\boldsymbol{H}_v$ is the measurement matrix for velocity aiding, $\boldsymbol{w}_{k-1}$ is the process noise, $\boldsymbol{\eta}_{v,k}$ is the velocity measurement noise, $z_{v,k}$ is the velocity error derived from the velocity estimate $\hat{\boldsymbol{v}}_k^n$, and

$$\begin{aligned} \boldsymbol{F}_k &= \begin{bmatrix} \boldsymbol{I}_{3\times3} & \boldsymbol{O}_{3\times3} & \boldsymbol{O}_{3\times3} \\ \boldsymbol{S}_k \cdot \Delta t & \boldsymbol{I}_{3\times3} & \boldsymbol{O}_{3\times3} \\ \boldsymbol{O}_{3\times3} & \boldsymbol{I}_{3\times3} \cdot \Delta t & \boldsymbol{I}_{3\times3} \end{bmatrix}, \\ \boldsymbol{H}_v &= \begin{bmatrix} \boldsymbol{O}_{3\times3} & \boldsymbol{I}_{3\times3} & \boldsymbol{O}_{3\times3} \end{bmatrix}, \end{aligned}$$

where Δt is the sampling period, $\boldsymbol{I}_{3\times3}$ is a 3×3 identity matrix, $\boldsymbol{O}_{3\times3}$ is a 3×3 zero matrix; $\boldsymbol{S}_k$ is the skew-symmetric matrix of the specific force $\boldsymbol{f}^n$ and $\boldsymbol{f}^n = \boldsymbol{C}_b^n \boldsymbol{f}^b$.

The process and measurement noises are assumed to be independent Gaussian white noises, and then a Kalman-type filter with one measurement update and one observation update can be implemented to accomplish the ZUPT-aided INS. During the ZUPT period of each subsystem, the estimate of $\delta\boldsymbol{x}_k$ can be used to correct the raw estimate of $\boldsymbol{x}_k$, and therefore a closed-loop ZUPT-aided INS is completed. For a more detailed description, see our earlier work [27].

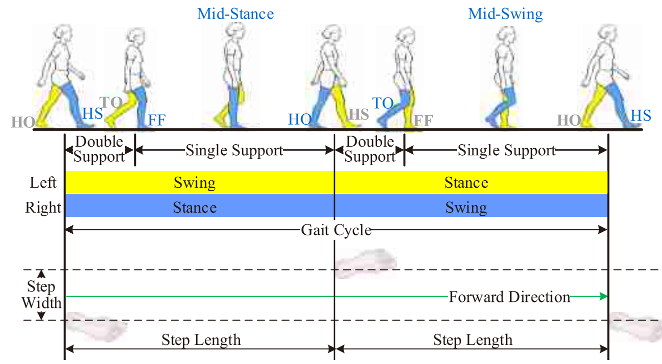

Fig. 3. Spatial-temporal gait parameters.

III. Gait Parameter for Position Updates

As the two INSs are non-collocated, they will track different points of user's body; as human body is non-rigid, the relative positions of the subsystems are not fixed. There is a question about how to fuse the navigation solutions of these subsystems. Fortunately, the feet separation relates to the spatial gait parameters that can be modeled and estimated [20]. To obtain the gait parameters, we need to detect the gait phases first.

A. Gait Phase Detection

As shown in Fig. 3, there are four typical events in one normalized gait cycle: heel-strike (HS), foot-flat (FF), heel-off (HO), and toe-off (TO). Usually, a gait cycle is defined as the interval between two successive HS events of ipsilateral foot, while a step is defined as the interval between two successive HS events of alternate feet. The step establishes a connection between the two uncoupled foot-mounted INSs. A gait cycle can be divided into several phases by the gait events, from two to four or even more according to the specific purpose. In our study, a gait cycle is divided into two phases, i.e., a stance (HS to HO) and a swing (HO to HS), where the HS to HO events are of the same foot in terms of single-gait analysis.

As the IMUs are placed on the user's heels, the inertial measurements should feature periodic patterns according to the gait cycle, which are adequate for gait analysis. A segment

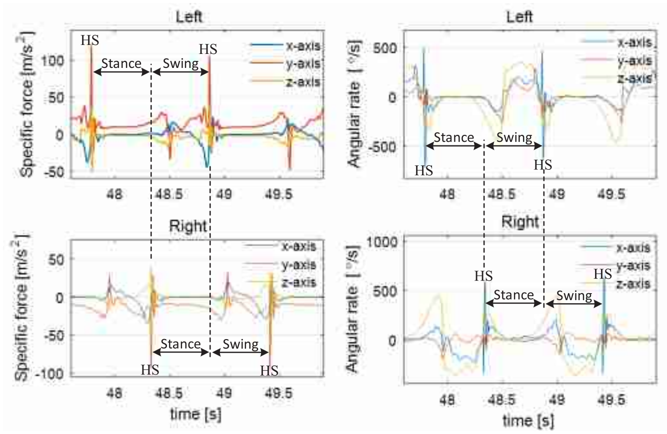

Fig. 4. Inertial measurements with key gait events and gait phases.

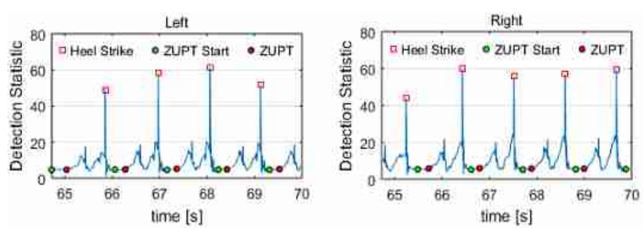

Fig. 5. Results of gait division and gait detection.

of raw measurements is shown in Fig. 4, together with the key gait events and corresponding gait phases. The measurements exhibit sudden spikes when the HS events occur, especially for the acceleration, which means that the HS events have more prominent features than the others for gait event indication. Since the HO events of rear foot always coincide with the HS events of the front foot, this paper detects the gait phases using the data from both feet jointly through dual-gait analysis. Specifically, a stance phase starts with the HS event of supporting foot, but ends with the HS event of contralateral foot, and vice versa. This delimitation of gait phase coincides with the definition of step.

The HS event is followed by the FF event, from which the foot is flat on the ground until subsequent HO event. During this period, the angular rate is near to zero, while the acceleration becomes constant and remains around gravity. These patterns facilitate the detection of the key gait events and the concerned gait phases. A peak detection method is used to detect the HS events, whereas a flat zone detection method is used to delimit the ZUPT periods. The detection results are shown in Fig. 5. It can be seen that the ZUPT period corresponds to about 25% to 30% of a gait cycle, which is deemed sufficient for ZUPT technique to correct the navigation errors, considering a cycle time of 1 s to 1.2 s (for an adult walking at normal speed).

B. Step Length Estimation

When the gait phases of each foot are correctly detected, the gait parameters between two feet will be derived accordingly. In this paper, the feet separation is suggested to be represented by a 3D relative position vector that relates to

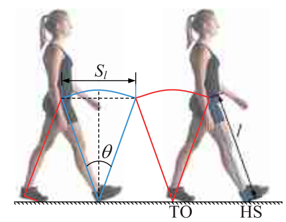

Fig. 6. Inverted pendulum model of human walking.

the spatial step parameters, i.e., step length, step width and step elevation, which corresponds to the travelled distance in the forward, lateral and vertical directions respectively at the end of a step. In this sense, the often-mentioned upper bound on feet separation is equal to the magnitude of this relative vector when both feet are on the ground, as seen in Fig. 3.

Note that the step elevation defined here is different to the known step height that defined as the maximum heel elevation over a step. Among these three components, the step width variability is not obvious, the step elevation depends on the ground condition, which is equal to zero during a horizontal walking or equal to the stair height when ascending or descending stairs, whereas the step length varies considerably and needs to be calculated for each step of each individual.

Many factors have an influence on step length, such as leg length, walking speed, and gait type. Hence, the step length has different values among the literature sources. As stated in [28], the step length is about 0.75 m for healthy adults walking at their self-selected speed of about 1.4 m/s; whereas in [29], the average step length varies for males and females, which is around 0.79 m for males and 0.66 m for females. These figures are less than the empirically predefined upper bound on feet separation. Therefore, for a realistic step length estimation, it is necessary to consider the natural variability of individual gait pattern.

With anthropometric and biomechanical considerations specific to user's gait, it is possible to deduce the step length and thereby making the two INSs coupled. In this paper, in order to make no modification to the original system, human gait is described by an inverted pendulum model of a kneeless biped on the sagittal plane, as shown in Fig. 6. The step length S_l can be presented as the forward displacement of the body's COM during the stance phase of the contralateral rear foot that acts as a supporting pivot. Thus, step length computation begins with the HS event of the rear foot and ends with the HS event of the front foot, according to the delimitation of stance phase in this paper.

As is known, the attitude of an object can be equivalently represented by Euler angles, rotation matrix, and quaternion. The quaternion can be represented in an axis-angle form as

$$\boldsymbol{q} = \cos(\frac{\theta}{2}) + \boldsymbol{u}\sin(\frac{\theta}{2}), \tag{4}$$

where $\boldsymbol{u} \in \mathbb{R}^3$ is the unit vector along the rotation axis, and θ is the rotation angle.

Define $\boldsymbol{q}_1$ and $\boldsymbol{q}_2$ as the start and end quaternions of the supporting foot during a step, respectively. The attitude change over the step can be determined by

$$\begin{cases} \boldsymbol{q} = \boldsymbol{q}_1 \otimes \boldsymbol{q}_2^* \\ \theta = 2\cos^{-1}(\boldsymbol{q}[1]), \end{cases} \tag{5}$$

where $\boldsymbol{q}_2^*$ denotes the conjugate of $\boldsymbol{q}_2$, and $\boldsymbol{q}[1]$ denotes the first term of $\boldsymbol{q}$.

Then, a mathematical model driven by indirect gyroscope data can be adopted to estimate the successive step lengths by

$$S_l = 2l\sin(\frac{\theta}{2}), \tag{6}$$

where l acts as the pendulum length approximated by user's leg length, and $\frac{\theta}{2}$ acts as the amplitude that the pendulum swings away from vertical.

As seen in (6), two parameters are involved in this gyroscope-based estimator, where l is a constant that has to be specified for each individual, whereas θ is a variable that is related to the INS-derived attitude parameters. The main advantages of this step length estimator are as follows:

1) it requires no previous parametric adjustment or calibration from the walking data of every individual;

2) it complies with the dual-sensor configuration of the original system setup with one IMU on each foot;

3) it requires little additional computation, as the calculation of attitude is a necessary step for INS mechanism;

4) is uses gyroscope measurements solely, which has a lower SNR (signal-to-noise ratio) than that of the accelerometer measurements due to the specificity of foot movement.

IV. ZUPT-Aided INS With Position Updates

A. Sensor Fusion Structure

With knowledge of gait parameters, the separation of two feet can be expressed by the three components between them rather than an absolute distance. Relative position updates can be implemented to fuse the positions of the two foot-mounted INSs at person level, which is supposed to further improve the system accuracy in addition to ZUPT. The position estimate of a target footprint can be obtained by two ways:

1) the ZUPT-aided INS allows a position propagation at each time instant with some uncertainty;

2) the latest step supported by the contralateral foot suggests a possible position with some uncertainty.

These estimations can be fused with a Kalman-type filter to limit the uncertainty growth. Fig. 7 shows the data flow of the dual-sensor fusion structure. The position update is triggered whenever the relative position observation is available.

B. Sensor Fusion Mechanism

For the dual-sensor configuration, each subsystem has its own error state $\delta\boldsymbol{x}_{i,k} = [\delta\boldsymbol{\varphi}_{i,k}, \delta\boldsymbol{v}_{i,k}^n, \delta\boldsymbol{p}_{i,k}^n]^T \in \mathbb{R}^9$ estimated by a ZUPT-aided INS, where i ($i = 1, 2$) denotes the i-th system. Defined the relative position vector as $\Delta\boldsymbol{p}_k^b$, which is derived in the b-frame that determined by the rear foot. To perform the position updates in n-frame, a rotation must be applied to yield the position vector $\Delta\boldsymbol{p}_k^n$. The position measurement update equation can be expressed as

$$z_{p,k} = \boldsymbol{H}_p \cdot \delta\boldsymbol{x}_k + \boldsymbol{\eta}_{p,k}, \tag{7}$$

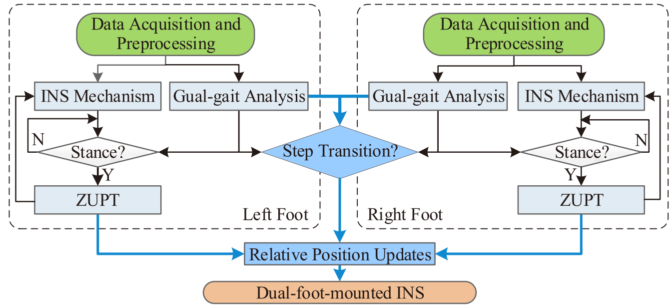

Fig. 7. Structure of the Dual-foot-mounted INS.

(a) (b)

Fig. 8. Hardware setup of the foot-mounted INS implementation. (a) System assembly without lid. (b) Entire system assembly.

where $z_{p,k}$ is the position error observation, $\boldsymbol{H}_p$ is the measurement matrix for position aiding, $\boldsymbol{\eta}_{p,k}$ is the position measurement noise, and

$$z_{p,k} = (\hat{\boldsymbol{p}}_{1,k}^n - \hat{\boldsymbol{p}}_{2,k}^n) - \Delta\boldsymbol{p}_k^n,$$
$$\boldsymbol{H}_p = [\boldsymbol{O}_{3\times3} \quad \boldsymbol{O}_{3\times3} \quad \boldsymbol{I}_{3\times3}],$$

where $\hat{\boldsymbol{p}}_{1,k}^n$ and $\hat{\boldsymbol{p}}_{2,k}^n$ are the position estimates of the front and rear foot, respectively.

There is no standard way of feeding such observations to a Kalman-type filter. This paper presents a Kalman framework with one time update and two measurement updates to handle the error models in (3) and (7), where the first measurement refers to the zero velocity of each foot while the second measurement refers to the relative position between two feet.

V. Experiment

In this section, the experimental setup is first described, then the results of the experiments are presented and analyzed, and finally some discussions on the experimental results are made.

A. Experimental Setup

The experiments were conducted by four healthy adults in an open stadium. Each subject was equipped with two inertial sensors, one on each heel. The sensor used is ADIS16448 from Analog Devices [30], which includes a triaxial gyroscope with a range of ±1000 °/s and a triaxial accelerometer with a range of ±18 g. The bandwidth and sample rate of the sensor is 330 Hz and 400 Hz, respectively. The dimensions of each system assembly are 4.50 cm × 3.50 cm × 2.25 cm, as shown in Fig. 8. The data collected during experiments were stored in an internal memory and then transferred to an external computer for further processing.

Prior to each walking, the system was kept stationary for a short while to perform initial alignment and calibration. Two types of walking trajectories were planned: a straight line

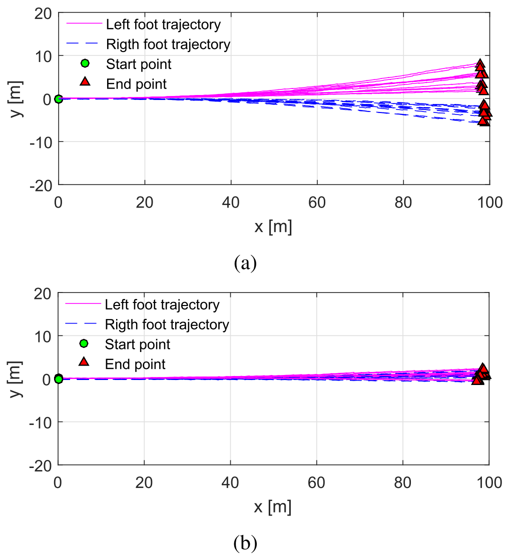

Fig. 9. Estimated trajectories for walking along a straight line. (a) Without the relative position updates. (b) With the relative position updates.

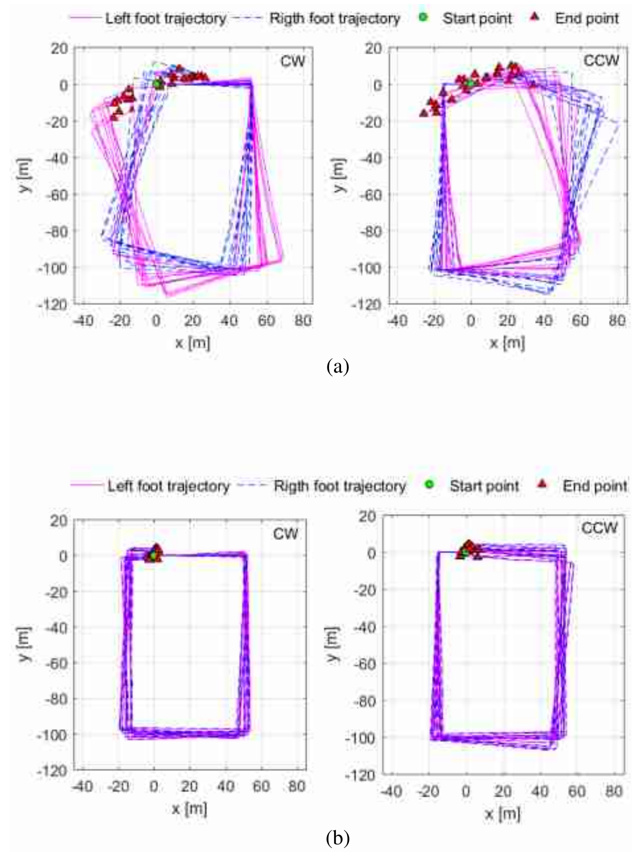

Fig. 10. Estimated trajectories for walking along a big rectangle. (a) Without the relative position updates. (b) With the relative position updates.

trajectory (Test #1) and a rectangular trajectory (Test #2). The subjects were allowed to turn freely and walk at self-selected comfortable speeds. For each traveled step, the step length provides the forward distance, the step width is assumed to equal the user's shoulder width, and the vertical distance is assumed zero on level ground.

B. Experimental Results

For all experiments, the start position corresponds to the origin of n-frame, and the initial heading is along X-axis.

1) Straight Line Trajectory: Experiments were first conducted along a 100 m straight line trajectory that parallel to a stadium track. Each subject was asked to repeat the experiment three times with same initial orientation, and 12 datasets were collected at this stage. Fig. 9 shows the walking trajectories estimated by the dual-foot-mounted ZUPT-aided INS with and without the relative position updates, respectively.

Straight line trajectory was chosen to demonstrate how large the lateral position errors would be due to the system heading drift, and what system improvements can be achieved by applying the relative position updates. As the step length estimator works well for straight line walking, the estimated trajectories in Fig. 9(b) coincide well with the ground truth and the actual dual-foot motion.

2) Big Rectangular Trajectory: To further evaluate system performance, experiments were then conducted on a football field of the stadium. The football field is covered with green grass and has a standard size of 105 m × 68 m. The trajectory is designed along the rectangular periphery of the football field, which is 346 m long in total. Each subject was asked to repeat the experiment three times with clockwise (CW) initial orientation and three times with counterclockwise (CCW) initial orientation. At this stage, 24 datasets were collected, half with CW turns and half with CCW turns. Fig. 10 shows the walking trajectories estimated with and without the relative position updates, respectively.

The soft grass surface raises a strong challenge to gait phase detection. It is difficult for the feet to show zero velocities during their stance phase, due to the presence of measurement fluctuations when they contact the grass. This will add more modeling errors that related to ZUPT, and thereby lead to significant heading drift, as can be seen in Fig. 10(a).

The closed-loop trajectories were chosen to cancel out the effects of initial heading alignment errors. At the end of each trial, the feet were expected to return to their start positions. As seen in Fig. 10(b), the final position errors and the heading drifts are greatly bounded, as well as the relative position error between the two feet.

3) Overall System Performance: The system performance is evaluated with two metrics, i.e., final foot separation E_s and final position error E_p, which are defined as

$$\begin{aligned} E_s &= \left\| \hat{\boldsymbol{P}}^n_{1,end} - \hat{\boldsymbol{P}}^n_{2,end} \right\| \\ E_p &= \left\| \hat{\boldsymbol{P}}^n_{i,end} - \boldsymbol{P}^n_{i,end} \right\|, \end{aligned} \tag{8}$$

where $\|\cdot\|$ is the 2-norm of a vector, i $(i = 1, 2)$ denotes the i-th system, $\hat{\boldsymbol{P}}^n_{i,end}$ is the estimated end position, and $\boldsymbol{P}^n_{i,end}$ is the true end position.

The final position error is calculated for each foot. Table I summarizes the system performance and improvement for all experiments, in terms of the mean and standard deviation of the performance metrics. The experimental results show that the proposed dual-sensor fusion method improves the system

TABLE I
OVERALL SYSTEM PERFORMANCE FOR ALL EXPERIMENTS (m)

Test		Relative Position Update	Foot Separation	Position Error	
				Left Foot	Right Foot
#1		Without	7.33±3.31	4.41±2.21	2.98±1.45
		With	0.42±0.14	1.59±0.49	1.46±0.58
#2	CW	Without	33.18±14.02	18.95±7.00	16.32±7.40
		With	0.37±0.09	2.67±1.05	2.63±1.05
	CCW	Without	31.32±16.34	14.55±10.09	19.36±8.03
		With	0.32±0.05	3.42±1.88	3.54±1.91

performance and reduces the heading drift to a very low level, which is achieved by imposing a user-specific and gait-specific relative position updates to the uncoupled foot-mounted INSs and making them relate to each other as they actually do.

C. Discussion

As shown in Fig. 9, the step length estimator works well for straight line walking. However, there are some types of motions that cause deviations from ideal straight line travel, such as swaying, curving, and turning. As pedestrians do not walk exactly straight, swaying can be defined as the motion that is intended to be straight but not perfectly straight due to the nature of walking sway [31]. As swaying has minor perceived amplitude, a simple heading threshold would be sufficient to distinguish it from curving or turning. When a curving or turning motion is perceived, the relative position updates will be suspended temporarily.

As seen in Fig. 10, for a closed-loop trajectory, the final position error is often chosen as a performance metric when little ground truth is available. However, even small return position error is achieved at the end of the trial, large relative position errors between the feet may exist during the walking process. In this sense, the proposed dual-sensor method not only provides a means for reducing the heading drifts, but also provides ideas for evaluating the system more rigorously and comprehensively. Therefore, more reasonable metrics should be explored to accurately evaluate the system performance.

The foot-mounted INS works as a foot tracker, which locates the pedestrian through foot movement. By means of dual-gait analysis, step length estimation, as well as the periodic velocity and position updates, the estimated trajectories coincide well with the ground truth and the actual dual-foot motion. Thus, the dual-foot-mounted INS has potential use in many applications based on the spatial-temporal gait parameters, not only pedestrian localization and navigation, but also gait analysis, sport training, biological recognition, motion capture, etc.

VI. CONCLUSION AND FUTURE WORK

This paper has presented a multi-sensor fusion approach to reduce the heading drift for foot-mounted INS. Based on an inverted pendulum model, the step length is estimated to relate the uncoupled and non-collocated INSs to each other. To fuse the relative position information, a person level position updates is performed in addition to the commonly used foot level velocity updates. Therefore, an Kalman-type filter is presented to estimate the INS error with one time update and two measurement updates. The experimental results show that the heading drift is effectively reduced and the captured dual-foot motion is closer to its actual process.

In future work, we will evaluate our method with more gait patterns, such as turning, running, sidestepping, walking backwards, and ascending or descending stairs. This will pose new practical challenges to gait analysis and gait model, as some types of gait events may not occur or the order of gait events may change. Moreover, we will consider storing/processing data on smartphones or additionally using smartphones as another source of sensed data to fuse, to take advantage of the various sensors and processing resources of these ubiquitous smart mobile devices, as described in [32] and [33].

REFERENCES

[1] A. Vanclooster, N. Van de Weghe, and P. De Maeyer, "Integrating indoor and outdoor spaces for pedestrian navigation guidance: A review," *Trans. GIS*, vol. 20, no. 4, pp. 491–525, 2016.

[2] N. Raveendranathan *et al.*, "From modeling to implementation of virtual sensors in body sensor networks," *IEEE Sensors J.*, vol. 12, no. 3, pp. 583–593, Mar. 2012.

[3] N. Kitagawa and N. Ogihara, "Estimation of foot trajectory during human walking by a wearable inertial measurement unit mounted to the foot," *Gait Posture*, vol. 45, pp. 110–114, Mar. 2016.

[4] P. Chen, Y. Kuang, and X. Chen, "A UWB/improved PDR integration algorithm applied to dynamic indoor positioning for pedestrians," *Sensors*, vol. 17, no. 9, p. 2065, 2017.

[5] D. Taniuchi and T. Maekawa, "Automatic update of indoor location fingerprints with pedestrian dead reckoning," *ACM Trans. Embedded Comput. Syst.*, vol. 14, no. 2, pp. 1–23, 2015.

[6] L. Ojeda and J. Borenstein, "Non-GPS navigation for security personnel and first responders," *J. Navigat.*, vol. 60, no. 3, pp. 391–407, Sep. 2007.

[7] R. Gravina *et al.*, "Cloud-based Activity-aaService cyber–physical framework for human activity monitoring in mobility," *Future Gener. Comput. Syst.*, vol. 75, pp. 158–171, Oct. 2017.

[8] G. Fortino, R. Giannantonio, R. Gravina, P. Kuryloski, and R. Jafari, "Enabling effective programming and flexible management of efficient body sensor network applications," *IEEE Trans. Human-Mach. Syst.*, vol. 43, no. 1, pp. 115–133, Jan. 2013.

[9] H. Zhao, Z. Wang, H. Shang, W. Hu, and Q. Gao, "A time-controllable Allan variance method for MEMS IMU," *Ind. Robot*, vol. 40, no. 2, pp. 111–120, 2013.

[10] H. Zhao, Z. Wang, Q. Gao, M. M. Hassan, and A. Alelaiwi, "Smooth estimation of human foot motion for zero-velocity-update-aided inertial pedestrian navigation system," *Sensor Rev.*, vol. 35, no. 4, pp. 389–400, 2015.

[11] T. Brand and R. Phillips, "Foot-to-foot range measurement as an aid to personal navigation," in *Proc. 59th Inst. Navigat. Annu. Meeting*, Albuquerque, NM, USA, 2003.

[12] R. Gravina, P. Alinia, H. Ghasemzadeh, and G. Fortino, "Multi-sensor fusion in body sensor networks: State-of-the-art and research challenges," *Inf. Fusion*, vol. 35, pp. 68–80, May 2017.

[13] J. C. Alvarez, R. C. Gonzalez, D. Alvarez, A. M. Lopez, and J. Rodriguez-Uria, "Multisensor approach to walking distance estimation with foot inertial sensing," in *Proc. 29th Annu. Int. Conf. IEEE Eng. Med. Biol. Soc.*, Aug. 2007, pp. 5719–5722.

[14] G. V. Prateek, R. Girisha, K. V. S. Hari, and P. Händel, "Data fusion of dual foot-mounted INS to reduce the systematic heading drift," in *Proc. 4th Int. Conf. Intell. Syst., Modelling Simulation*, 2013, pp. 208–213.

[15] I. Skog, J.-O. Nilsson, D. Zachariah, and P. Händel, "Fusing the information from two navigation systems using an upper bound on their maximum spatial separation," in *Proc. Int. Conf. Indoor Positioning Indoor Navigat.*, 2010, pp. 1–5.

[16] R. Girisha, G. V. Prateek, K. V. S. Hari, and P. Händel, "Fusing the navigation information of dual foot-mounted zero-velocity-update-aided inertial navigation systems," in *Proc. Int. Conf. Signal Process. Commun.*, 2014, pp. 1–6.

[17] D. Zachariah, I. Skog, M. Jansson, and P. Händel, "Bayesian estimation with distance bounds," *IEEE Signal Process. Lett.*, vol. 19, no. 12, pp. 880–883, Dec. 2012.

[18] J.-O. Nilsson, D. Zachariah, I. Skog, and P. Händel, "Cooperative localization by dual foot-mounted inertial sensors and inter-agent ranging," *EURASIP J. Adv. Signal Process.*, 2013, Art. no. 164.

[19] W. Shi, Y. Wang, and Y. Wu, "Dual MIMU pedestrian navigation by inequality constraint Kalman filtering," *Sensors*, vol. 17, no. 2, pp. 427–439, 2017.

[20] J. B. Bancroft, G. Lachapelle, M. E. Cannon, and M. G. Petovello, "Twin IMU-HSGPS integration for pedestrian navigation," in *Proc. 21st Int. Tech. Meeting Satell. Division Inst. Navigat.*, 2008, pp. 1377–1387.

[21] K. Tong and M. H. Granat, "A practical gait analysis system using gyroscopes," *Med. Eng. Phys.*, vol. 21, no. 2, pp. 87–94, 1999.

[22] K. Aminian, B. Najafi, C. Büla, P. F. Leyvraz, and P. Robert, "Spatio-temporal parameters of gait measured by an ambulatory system using miniature gyroscopes," *J. Biomech.*, vol. 35, no. 5, pp. 689–699, 2002.

[23] E. Allseits, V. Agrawal, J. Lučarević, R. Gailey, I. Gaunaurd, and C. Bennett, "A practical step length algorithm using lower limb angular velocities," *J. Biomech.*, vol. 66, pp. 137–144, Jan. 2018.

[24] J. Jahn, U. Batzer, J. Seitz, L. Patino-Studencka, and J. G. Boronat, "Comparison and evaluation of acceleration based step length estimators for handheld devices," in *Proc. Int. Conf. Indoor Positioning Indoor Navigat.*, 2010, pp. 1–6.

[25] D. Alvarez, R. C. González, A. López, and J. C. Alvarez, "Comparison of step length estimators from weareable accelerometer devices," in *Proc. 28th Annu. Int. Conf. IEEE Eng. Med. Biol. Soc.*, Aug./Sep. 2006, pp. 5964–5967.

[26] Y. Qi, C. B. Soh, E. Gunawan, K.-S. Low, and R. Thomas, "Estimation of spatial-temporal gait parameters using a low-cost ultrasonic motion analysis system," *Sensors*, vol. 14, no. 8, pp. 15434–15457, 2014.

[27] Z. Wang, H. Zhao, S. Qiu, and Q. Gao, "Stance-phase detection for ZUPT-aided foot-mounted pedestrian navigation system," *IEEE/ASME Trans. Mechatronics*, vol. 20, no. 6, pp. 3170–3181, Dec. 2015.

[28] P. H. Sessoms, "Step by step: A study of step length in able-bodied persons, race walkers, and persons with amputation," Ph.D. dissertation, Dept. Biomed. Eng., Northwestern Univ., Evanston, IL, USA, 2008.

[29] T. Yamaguchi, S. Hatanaka, and K. Hokkirigawa, "Effect of step length and walking speed on traction coefficient and slip between shoe sole and walkway," *Tribol. Online*, vol. 3, no. 2, pp. 59–64, 2008.

[30] Analog Devices. *ADIS16448*. Accessed: May 27, 2018. [Online]. Available: http://www.analog.com/en/products/sensors-mems/inertial-measurement-units/adis16448.html

[31] J. Borenstein, L. Ojeda, and S. Kwanmuang, "Heuristic reduction of gyro drift for personnel tracking systems," *J. Navigat.*, vol. 62, no. 1, pp. 41–58, 2009.

[32] M. Hirsch, C. Mateos, and A. Zunino, "Augmenting computing capabilities at the edge by jointly exploiting mobile devices: A survey," *Future Gener. Comput. Syst.*, vol. 88, pp. 644–662, Nov. 2018.

[33] M. Hirsch, J. M. Rodríguez, C. Mateos, and A. Zunino, "A two-phase energy-aware scheduling approach for CPU-intensive jobs in mobile grids," *J. Grid Comput.*, vol. 15, no. 1, pp. 55–80, 2017.

Hongyu Zhao received the B.Sc., M.Sc., and Ph.D. degrees in automatic control from the Dalian University of Technology, Dalian, China, in 2007, 2009, and 2015, respectively.

She is currently a Lecturer with the School of Control Science and Engineering and a Post-Doctoral Researcher with the School of Computer Science and Technology, Dalian University of Technology. Her current research interests include pedestrian navigation, indoor localization, inertial navigation and positioning, and gait analysis.

Zhelong Wang (M'04–SM'18) received the B.S. and M.S. degrees in automatic control from the Dalian University of Technology, Dalian, China, in 1996 and 1999, respectively, and the Ph.D. degree in robotics from the University of Durham, U.K., in 2003.

In 2004, he joined the School of Electronic and Information Engineering, Dalian University of Technology, where he is currently a Professor. His research interests include robotics, intelligent control, mechatronics, body sensor networks, and machine learning.

Dr. Wang was elected into the Liaoning Province Hundred, Thousand, and Ten Thousand Talent Project in 2009. Hereceived the Research Award from the Audi Foundation in 2008, the Dalian Excellent IT Teacher Award in 2008, and the First Prize from the Liaoning Province Natural Science Award (Academic Paper Program) in 2009.

Sen Qiu received the B.Sc. and Ph.D. degrees in automatic control from the Dalian University of Technology, Dalian, China, in 2008 and 2016, respectively.

He was a Visiting Researcher with the Department of Computer Science and Electronic Engineering, University of Essex, Colchester, U.K., from 2013 to 2014. He is currently a Lecturer with the Dalian University of Technology. His current research interests include gait analysis, body sensor networks, and pattern recognition.

Yanming Shen received the B.S. degree in automation from Tsinghua University, Beijing, China, in 2000, and the Ph.D. degree from the Department of Electrical and Computer Engineering, New York University Tandon School of Engineering, Brooklyn, in 2007.

He is currently a Professor with the School of Computer Science and Technology, Dalian University of Technology, China. His general research interests include packet switch design, data center networks, peer-to-peer video streaming, algorithm design, analysis, and optimization. He was a recipient of the 2011 Best Paper Award for Multimedia Communications from the IEEE Communications Society.

Luyao Zhang received the B.S. degree in automation from Henan Polytechnic University, Jiaozuo, China, in 2016. He is currently pursuing the M.S. degree with the School of Control Science and Engineering, Dalian University of Technology, Dalian, China.

His research interests include indoor localization, gait analysis, and pedestrian navigation.

Kai Tang is currently a Professor with the First Affiliated Hospital of Dalian Medical University, Dalian, China.

Giancarlo Fortino (SM'12) received the Ph.D. degrees in computer engineering from the University of Calabria (Unical), Italy, in 1995 and 2000, respectively. He is currently a Professor of Computer Engineering with the Department of Informatics, Modeling, Electronics, and Systems, Unical.

He is also an Adjunct Professor with the Wuhan University of Technology, Wuhan, China, and a Senior Research Fellow with the Italian National Research Council ICAR Institute. He is also a Co-Founder and the CEO of SenSysCal S.r.l., a Unical spin-off focused on innovative IoT systems. He has authored over 350 papers international journals, conferences, and books. His research interests include agent-based computing, wireless (body) sensor networks, and Internet of Things. He is currently a member of the IEEE SMCS BoG. He is also the Chair of the IEEE SMCS Italian Chapter.